



HAL
open science

Introducing 'trident': a graphical interface for discriminating groups using dental microwear texture analysis

Ghislain Thiery, Arthur Francisco, Margot Louail, Emilie Berlioz, Cécile Blondel, Noël Brunetière, Anusha Ramdarshan, Axelle Ec Walker, G Merceron

► To cite this version:

Ghislain Thiery, Arthur Francisco, Margot Louail, Emilie Berlioz, Cécile Blondel, et al.. Introducing 'trident': a graphical interface for discriminating groups using dental microwear texture analysis. 2024. hal-04222508v2

HAL Id: hal-04222508

<https://hal.science/hal-04222508v2>

Preprint submitted on 23 Jun 2024

HAL is a multi-disciplinary open access archive for the deposit and dissemination of scientific research documents, whether they are published or not. The documents may come from teaching and research institutions in France or abroad, or from public or private research centers.

L'archive ouverte pluridisciplinaire **HAL**, est destinée au dépôt et à la diffusion de documents scientifiques de niveau recherche, publiés ou non, émanant des établissements d'enseignement et de recherche français ou étrangers, des laboratoires publics ou privés.



Distributed under a Creative Commons Attribution - NonCommercial 4.0 International License

1 **Introducing ‘trident’: a graphical interface**
2 **for discriminating groups using dental**
3 **microwear texture analysis**
4

5 Thiery G.^{1,2}, Francisco A.³, Louail M.¹, Berlioz E.^{1,4}, Blondel C.¹, Brunetière N.³, Ramdarshan
6 A.¹, Walker A. E. C.¹, Merceron G.¹

7
8 1. Laboratoire PALEVOPRIM, UMR 7262, CNRS & Université de Poitiers, France

9 2. Center for Evolutionary Origins of Human Behavior EHUB, Kyoto University Museum,
10 Japan

11 3. Institut Pprime, UPR CNRS 3346, Université de Poitiers, France

12 4. EvoAdapta Group, University of Cantabria, Santander, Spain
13
14
15

16 Corresponding authors: A. Francisco, G. Merceron

17 gildas.merceron@univ-poitiers.fr

18 arthur.francisco@univ-poitiers.fr
19

20 **Abstract**

21

22 This manuscript introduces trident, an R package for performing dental microwear texture
23 analysis and subsequently classifying variables based on their ability to separate discrete
24 categories. Dental microwear textures reflecting the physical properties of the food, it
25 highlights the feeding ecology of a given species and then niche partitioning when considering
26 multi-specific communities. The trident package comes with independent functions and a user
27 interface, trident, enabling easy and fast proficiency. It can import .SUR files, then remove
28 aberrant peaks and possibly polynomial surfaces. Next, it can measure up to 24 texture
29 parameters and their statistics of heterogeneity generating by then 384 variables . It also
30 ranks any number of variables using five different methods, displays the results in multivariate
31 analyses, and exports the results in R, providing access to its large asset of libraries.

32 We then present these features in three case studies, showing how trident helps answer
33 questions commonly investigated by paleontologists and archaeologists. In the first case
34 study, we separate four groups of domestic pigs based on their dietary composition. In the
35 second case study, we identify microwear texture patterns in a large database of 15 primate
36 species and relate these patterns to biomechanical and ecological factors. The third case
37 study investigates the dental microwear textures of four extant ruminants to infer the diet of an
38 extinct antelope from the Pleistocene of Greece. These case studies show how trident can
39 leverage dental microwear texture analysis results.

40

41 Keywords: Diet inference; DMTA; Multivariate analysis

42 **Introduction**

43 **Fifty shades of dental microwear**

44 Dental microwear analysis has been a prominent method for investigating the diet of extant
45 and extinct species during the last 40 years (e.g., Walker et al., 1978; Kay, 1981; Teaford,
46 1985, 1988; Ungar, 1996; Teaford et al., 1996; Solounias & Semprebon, 2002; Merceron et al.,
47 2005; Merceron, Blondel, et al., 2005; Scott et al., 2005; Ungar et al., 2008; Rivals et al. 2011).
48 It is based on the observation that food leaves microscopic wear marks on dental wear facets,
49 and that those marks fade as the tooth wears, only to be replaced by new microwear marks
50 (Walker et al., 1978; Gordon, 1982; Teaford & Oyen, 1989; Winkler et al., 2020). The nature
51 (scratches or pits), size (small to large), and frequency of microwear depend on the food's
52 physical properties, mostly hardness, and abrasiveness, while their spatial distribution and
53 their anisotropy are related to chewing motions and food toughness (Teaford, 1988; Scott et
54 al., 2006; Teaford et al., 2020; Kubo & Fujita, 2021). This allows us to infer an animal's diet
55 during the last few weeks before its latest meal (Teaford & Oyen, 1989; Winkler et al., 2020).
56 Apart from diet, the role of exogenous soil mineral particles and environmental conditions in
57 dental microwear formation should not be minimized (Schulz-Kornas et al., 2019; Schulz-
58 Kornas et al., 2020). Grit is indeed reportedly harder than enamel tissue and more abrasive
59 than food particles (Sanson et al., 2007; Lucas et al., 2013). Still, controlled feeding
60 experiments on sheep have shown that differences in dental microwear texture better reflect
61 diet than the amount of exogenous particles (Merceron et al., 2016). Their digestive anatomy
62 explains this as ruminants remove the largest external grit from food while the finest particles
63 mimic organic amorphous silica (Clauss et al., 2023).

64

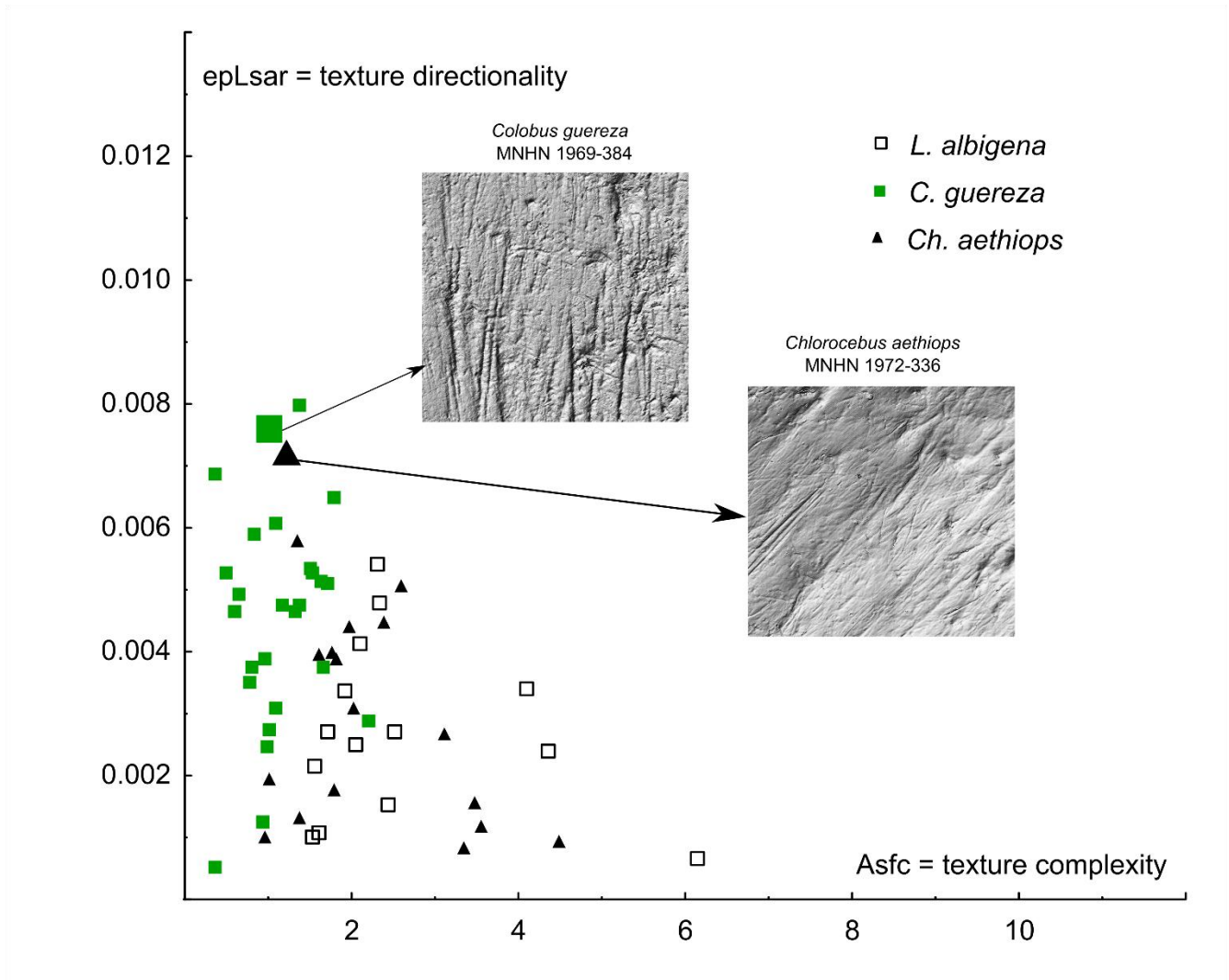
65 Initially, microwear analysis used scanning electronic or light microscopes to count pits and
66 scratches left by the food on the enamel surface. But despite a proven ability to separate

67 surfaces according to diet, this method is reliant on the tuning of light orientation, the counting
68 method, the observer experience, etc. (Grine et al., 2002; Galbany et al., 2005; Mihlbachler et
69 al., 2012). With the advent of high-resolution digitization techniques, new methods for
70 quantifying the three-dimensional surface texture have emerged. Scale Sensitive Fractal
71 Analysis (SSFA) uses surface parameters strongly correlated to food material properties,
72 such as surface scale roughness estimated from area-scale fractal complexity (Asfc) that
73 correlates to food hardness, or anisotropy (epLsar) that correlates to food toughness (Ungar
74 et al., 2003; Scott et al., 2005; Hua et al., 2020). A second approach, Surface Texture Analysis
75 (STA) consists of computing ISO-25178 area parameters (Schulz et al., 2010; Kaiser et al.,
76 2015). Both SSFA and STA methods belong to the larger field of dental microwear texture
77 analysis (DMTA). They have been used to investigate the diet of animals from a broad range
78 of species, including insectivorous mammals (Purnell et al., 2013) but also selacians (Weber
79 et al., 2021), lepidosaurians (Winkler et al., 2019) or dinosaurs (Sakaki et al., 2022; Winkler et
80 al. 2022).

81 **New methods, new challenges**

82 Despite their reliability, DMTA approaches are facing several methodological challenges. First,
83 they sometimes fail to separate specimens that an expert eye could visually tell apart using
84 the number of specific microwear marks (Fig. 1). This can be mitigated by using filters to
85 enhance the microwear versus the raw shape of the tooth surface, for instance by removing
86 the 2nd or 8th order polynomial of the surface using least square approximation (Francisco et
87 al., 2018a, 2018b). Failure to tell surfaces apart can also come from distinct structures
88 concealed in the average signal. One of the SSFA parameters can solve this issue by
89 estimating heterogeneity of complexity (HASfc, Scott et al., 2005, 2006). An alternative
90 approach is to consider a grid of standard number and size of cells and to measure every

91 parameter for each cell: the presence of distinct structures would increase the dispersion of
92 values, and could be detected using percentiles, minimal or maximal values, etc. (Francisco
93 et al., 2018a).



94

95 Figure 1. Biplot showing variations of dental microwear texture anisotropy (epLsar) and complexity (Asfc) on
96 crushing molar facets of wild-caught specimens belonging to three species of extant monkeys: the leaf-eating
97 colobine *Colobus guereza*, the fruit/seed-eating mangabey *Lophocebus albigena*, and the opportunistic vervets
98 *Chlorocebus aethiops*. There are quite significant overlaps between specific ranges. This is due to several
99 specimens for which although an expert eye can visually differentiate surfaces (200 × 200 μm), dental microwear
100 texture analysis cannot. For example, experts will count more wide scratches on the leaf-eating colobine (MNHN
101 1969-384) than on the opportunistic vervets (MNHN 1972-336). In contrast, DMTA fails to discriminate using
102 both anisotropy (epLsar) and complexity (Asfc). Using trident and specifically the subsampling method to explore
103 heterogeneity for all variables solves the issue.

104

105 Computing heterogeneity of DMTA variables helps track the most elusive structures, but it

106 tends to generate a “jungle of parameters” (Francisco et al., 2018b), that is, too many

107 variables to keep track of a given phenomenon. One way to bypass this issue is to compare
108 the variables' ability to discriminate groups, for instance using analyses of variance (ANOVAs)
109 to find which groups can be separated using post-hoc analysis such as Tukey's HSD or
110 Fisher's LSD. This analysis pipeline is very efficient and could separate animals according to
111 their diet in several studies (Francisco et al., 2018a, 2018b; Louail et al., 2021; Merceron et
112 al., 2021b).

113 Yet two more limitations can be identified. The first one concerns the repeatability of
114 measures, as the code was not accessible in previous works. The second limitation is the
115 ease of use since the pipeline made use of a combination of Fortran, Python, and R to collect
116 the data. Consequently, fine-tuning the nature of data collection and analysis was only
117 possible for people familiar with those languages. An open-source user interface would solve
118 both issues and make measuring, analyzing, and untangling DMTA data easier, faster, and
119 more intuitive for beginners.

120 Here, we introduce trident, a user interface, and its associated R source package trident for
121 measuring dental microwear textures and analyzing the discriminant ability of DMTA variables.
122 It can load .SUR files, remove abnormal peaks and measure 16 variables from 24 DMTA
123 parameters (for a total of 384 variables) on batches. The computed DMTA variables (along
124 with variables possibly added by the user on the source .txt file) can be classified according to
125 their ability to discriminate discrete categories such as species, diet, and any other categorical
126 variable. trident also comes with tools to perform univariate, bivariate, and multivariate
127 analysis. All the functions can be performed from the user interface. It is worth noting that
128 trident is free of access and the code is available to the scientific community.

129 We then showcase its functionalities using three case studies, representative of research
130 questions that could be answered using dental microwear analysis:

131 Case study A. Diet-related differences in dental microwear: The first case study is based
132 on a controlled feeding experiment involving a single omnivorous species (*Sus*
133 *domesticus*). Similarly to Louail et al. (2021), animals participated in trials only differing
134 in the dietary composition of their daily ration. The influence of diet on DMTA was then
135 quantified using trident.

136 Case study B. Meta-analysis of a large multi-species sample: The second case study is
137 based on a large sample grouping 260 specimens from 15 species of cercopithecoid
138 primates of Asia and Africa. We used trident to detect patterns related to species, their
139 tribe (Cercopithecini, Colobini, Papionini, and Presbytini), or their general diet
140 according to the literature.

141 Case study C. Comparison with extant species to infer the diet of extinct species: The
142 third case study is based on four sympatric species of ruminants from the Bauges
143 Natural Regional Park, French Alps. In a previous study, SSFA variables could find
144 differences between species, reflecting differences in dietary behavior and spatial use
145 (Merceron et al., 2021a). We used trident to explore the dental microwear textures of
146 this community and then used the most discriminating variables to make inferences on
147 the diet of *Gazellospira torticornis*, an extinct antelope from Greece (Hermier et al.,
148 2020).

149 **Material and Methods**

150 **Material**

151 ***Case study A: Diet-related differences in dental microwear***

152 The first case study is based on three of the feeding trials with domestic pigs (*Sus domesticus*)
153 detailed in Louail et al. (2021), to which was added another trial. The control group (N = 5)

154 was fed exclusively with a base diet composed of ground cereal and soy seeds. The three
155 other groups were also fed this base diet, with a supplement depending on their group:

- 156 • The *barley group* (N = 5) was fed 30 % of barley seeds.
- 157 • The *corn kernel* group (N = 5) was 20 % of corn (*Zea mays*) flour, supplemented with
158 20 % (as dry matter weight) of corn kernels.
- 159 • The *corn silage* group (N = 5) was fed 100 % of the base diet but had access to corn
160 silage at will.

161 We analyzed the deciduous upper fourth premolars of pigs aged between 6.5 and 9.5 months.

162 See Louail et al. (2021) for more details on the experiment.

163 ***Case study B: Meta-analysis of a large multi-species sample***

164 The second case study is based on skulls and jaws of extant cercopithecids from osteological
165 collections of Europe, Asia, and Africa (for a detailed listing of institutions, see Supplementary
166 Materials 1). A total of 260 casts of upper and lower second molars from 15 extant species
167 were obtained as detailed in previous studies (Merceron et al., 2021b; Thiery et al., 2021).
168 Each tribe of extant cercopithecids (Cercopithecini, Colobini, Papionini, and Presbytini) is
169 represented by at least 2 species (Supplementary Materials 1). Overall, the selected taxa
170 encompass a broad range of diets, from a large geographic range (see Rowe et al., 1996 and
171 citations therein).

172 ***Case study C Comparison with extant species to infer the diet of extinct species***

173 The Bauges Natural Regional Park is a typical subalpine massif located in the French Alps. In
174 the third case study, four extant ruminants from the Bauges have been investigated: *Cervus*
175 *elaphus*, a mixed-feeding species; *Capreolus capreolus*, a selective browser; *Ovis gmelini*
176 *musimon*, and *Rupicapra rupicapra*, two bovid species known to be mixed feeders. Mandibles
177 were collected at the same locality, during a short period (for more details, see Merceron et al.,

178 2021a), representing a hypothetical fossil assemblage composed of different species
179 occupying different small-scale habitats (open alpine grassland, bushland, shrubland,
180 deciduous, mixed, coniferous forests) in a common geographical range.

181 These four extant species were then compared to the extinct antelope *Gazellospira torticornis*
182 (Bovidae), from the Early Pleistocene of Greece. Specimens come from the site of Dafnero
183 and have been described by Hermier et al. (2020).

184 **Surface acquisition**

185 Each tooth surface was cleaned and molded as described in previous works (Louail et al.,
186 2021; Merceron et al., 2021a; Merceron et al., 2021b) and on the TRIDENT website
187 (<http://anr-trident.prd.fr/v/>). For case study A, we investigated both the shearing (phase I) and
188 crushing (phase II) dental facet of the very same tooth, whereas we focused on crushing
189 facets for case study B (primates) and on shearing facets for case study C (ruminants). Each
190 facet was scanned separately using a white-light confocal profilometer Leica DCM8, named
191 “TRIDENT”, with a 100× objective housed at the PALEVOPRIM lab, CNRS and University of
192 Poitiers, France (Leica Microsystems). All surfaces analyzed in the current study were pre-
193 processed with LeicaMap (v. 8.2; Leica Microsystems) following Merceron et al. (2016). The
194 procedure resulted in the obtention of .SUR files (saved as SUR version 7.2 or older), which
195 were then imported into trident. It is worth noting that alternative free-of-access software, such
196 as Gwyddion (<http://gwyddion.net/>) could be used to generate similar pre-treatments.

197 **DMTA with *trident***

198 ***Presentation of trident***

199 Here we introduce the R source package trident, which is devoted to measuring microwear
200 textures and classifying variables according to their discriminant power. It was implemented
201 on two levels:

202 (1) Functions that can be launched from the R console, for which detailed instructions can
203 be found in the metadata and the help files of the package.

204 (2) A shiny app named trident, which is launched from the console using the line
205 `trident.app()`. The app is a wrapper for the package functions, connecting them to
206 other packages for statistical analyses, multivariate analyses, or graphical rendering.

207 Below are summarized the functionalities of the interface used in the three case studies. The
208 reader can find a more detailed description of the interface in the user manual, provided as
209 supplementary materials (Supplementary Materials 2).

210 ***Dental microwear texture analysis (DMTA)***

211 Surfaces were first enhanced using the polynomial removal procedure; all procedures
212 mentioned below are detailed in Francisco, Brunetière et al. (2018). The primary surface S1
213 was first numerically and automatically cleaned of any abnormal peaks. Then, considering the
214 large-scale tooth surface geometry as an 8th-order polynomial (PS8), the latter was
215 subtracted via a least square approximation. This procedure was performed on surfaces of
216 the same size, as subtracting PS8 from smaller surfaces would remove larger amounts of
217 relief. The software also allows to remove of the 2nd order polynomial (PS2).

218 Afterward, DMTA variables were computed. The program can currently compute four families
219 of parameters (Table 1). The first one is complexity i.e., an estimation of the density of
220 microwear textures across scales. The second family is height, or parameters describing the
221 average height, its dispersion, and its variation over the surface whatever the location. The
222 third family is spatial parameters, which describe the distribution and nature of the textures.
223 The last family is topology, a combination of height and spatial parameters, measuring the
224 proportion of the surface above or below determined heights. A comparison of the height

225 parameter values found for trident and the Mountain-derived software is provided in the
226 supplementary information (supplementaryMaterial_Software comparisons.txt).

227

228 Table 1. DMTA parameters measured in trident

Parameter	Family	Significance	Description
Asfc2	Complexity	Area scale fractal complexity (#)	Asfc2 estimates roughness through scale-sensitive fractal analysis. Asfc2 would be low for smooth dental surfaces of leaf-eating colobine monkeys and high for rough surfaces frequent in hard seed-eating cercopithecine monkeys.
Sdar	Complexity	Relative area (developed area/projected area -1)	Sdar is higher for rough surfaces frequent in hard seed-eating cercopithecine monkeys than for smooth dental surfaces (of leaf-eating colobine monkeys; Sdar = 0 for a perfect horizontal plane surface)
Sa	Height	Arithmetic mean of the absolute of the heights (*)	Sa assesses surface roughness with low values for smooth dental surfaces of leaf-eating colobine monkeys and higher ones for rough surfaces frequent in hard seed-eating cercopithecine monkeys.
Sp	Height	Absolute of the largest height (*)	Sp is the height of the highest peaks, which is expected to be higher for rough surfaces found in species eating hard and brittle food items.
Sq	Height	Height standard deviation (*)	Sq is also expected to be higher for rough surfaces than smooth ones, such as the ones found for leaf-eating colobine monkeys.
Sv	Height	Absolute of the smallest height (*)	Sv is the height of the deepest pit, which is still expected to be higher for rough surfaces frequent in species eating hard and brittle food items.
Ssk	Height	Height skewness (*)	Ssk tends to be more negative for a surface with few deep pits as expected on dental surfaces of soft foliage and closer to 0 when a rough surface has many peaks and pits found in species eating hard and brittle food items.
Sku	Height	Height kurtosis (*)	Sku is expected to be higher (>>3) when the surface is smooth with few deep pits or/and high peaks, and close to 3 when peaks and pits have a wider range of height values around the mean
Sm	Height	Mean height (0 for the whole surface, but non-zero for its samples)	Useful when associated with statistics. It tells how the subsurface heights are distributed. Differences are expected with s
Smd	Height	Median height	Useful when associated with statistics. It tells how the subsurface heights are distributed.
Rmax	Spatial	Semi-major axis of the fACF ellipsis (**)	Rmax is higher for surfaces with long and parallel scratches usually found on molar facets of mammals avoiding hard and brittle foods that would require orthogonal crushing motion
Sal	Spatial	Semi-minor axis of the fACF ellipsis (**)	Sal is higher for wide and parallel scratches
Stri(*) = Str ⁻¹	Spatial	Rmax/Sal ratio (**)	Stri is high when there are numerous and long scratches.
b.sl	Spatial	Highest slope of fACF (**) at the distance rs from the origin ^β	Another way of quantifying the anisotropy. Highly correlated to Sal.
r.sl	Spatial	b.sl/s.sl ratio (**)	Another way of quantifying the anisotropy. Highly correlated to Stri.
s.sl	Spatial	Smallest slope of fACF (**) at the distance rs ^β from the origin	Another way of quantifying the anisotropy. Highly correlated to Rmax.
Std ^{EX}	Spatial	Texture direction	Std provides main orientation direction. Useful when combined with statistics, it shows how the direction of texture changes from one part of the surface to another.
Sk1, Sk2	Topology	Relative area of the surface above h1 ^{ββ} and h2 ^{ββ} respectively	Sk1 and Sk2 are higher for surfaces with many high heights.
Smc1, Smc2	Topology	Median relative area of the cells with heights exceeding h1 ^{ββ} and h2 ^{ββ} respectively	Smc1, Smc2 are higher for surfaces with many high heights arranged in large peaks.
Snb1, Snb2	Topology	Number of cells with heights exceeding h1 ^{ββ} and h2 ^{ββ} respectively	Snb1, Snb2 are higher for surfaces with many high heights arranged in thin peaks.
Sh	Topology	Percentage of quasi-horizontal faces (normal within a 4° cone)	Sh is low for rough surfaces and high for flat surfaces

229 ^{EX}, parameters excluded from the analysis; * ISO 25178 ; ** autocorrelation function at z=0.5 (Francisco et al.,
 230 2018a; 2018b) ; ^β maximum slope radius ; ^{ββ} h1 = 85 % of total height (Sv+Sp) and h2 = 95 % of total height
 231 (Sv+Sp)[#]; Area Scale Fractal Complexity is labeled Asfc2 because its calculation mode slightly differs from the
 232 Asfc computed in Scott et al., 2006).

233 Lastly, we estimated the heterogeneity for complexity, height, spatial, and topology variables.
234 The heterogeneity of a (dental) surface is related to the spatial distribution of its features: for
235 instance, a single pit in the enamel implies more heterogeneity than several pits uniformly
236 distributed through the enamel surface (Scott et al., 2006). Following Francisco, Brunetière et
237 al. (2018), trident uses a fast and intuitive approach for estimating heterogeneity: the surface
238 is divided into n grid cells, and DMTA parameters are computed for each grid cell. Then, the
239 distribution of DMTA parameters across grid cells is used to compute heterogeneity variables
240 e.g., mean Asfc2, maximal Asfc2, or 25th percentile of Asfc2 (Table 2). Note that this way of
241 assessing heterogeneity differs from SSFA parameters such as HAsfc (Box 1). In the end, a
242 total of 384 variables can be computed, giving a highly detailed description of dental
243 microwear textures. Out of these, 24 variables correspond to the 24 parameters from Table 1
244 measured on the whole surface, but the remaining 360 are estimates of surface heterogeneity.

245 trident does not allow to compute SSFA variables. Still, the user can find equivalents
246 among the 384 variables available in trident. For instance, Asfc can be approximated from
247 Asfc2, which also strongly correlates with Sdar. EpLsar, which is an SSFA estimate of
248 anisotropy, is related to spatial variables in trident. It is especially correlated with Rmax, Sal,
249 and Stri (Str-1), which are calculated with $s = 0.5$; value adapted for enamel wear surface
250 (Francisco et al. 2018a, 2018b). Note that trident can open and manage any other variables
251 (e.g.. SSFA, furrows, $\delta^{13}\text{C}$...) that a user might want to add to the source .txt file. This way, it
252 is easy to compare trident's variables with other parameters.

253 In each of the three case studies, all variables except minimal and maximal values
254 were calculated on 23 parameters (Std was excluded because it is scanning orientation-
255 dependent), for a total of 322 variables: this avoids measuring the effect of a single feature. To
256 assess the heterogeneity, the resampling statistics were calculated for a grid of 256 cells

257 (16×16) measuring 33 × 33 μm each (256 × 256 pixels) from the original surface measuring
258 200 × 200 μm (1551 × 1551 pixels).

259

260



261 Table 2. Heterogeneity variables.

Statistics	Description
min ^{EX}	Minimal value
max ^{EX}	Maximal value
sd	Standard deviation
mean	Arithmetic mean
med	Median
fst.05	5 th percentile
lst.05	95 th percentile
min.05	Mean of values under the 5 th percentile
max.05	Mean of values above the 95 th percentile
fst.25	1 st quartile
lst.25	3 rd quartile
min.25	Mean of values under the 1 st quartile
max.25	Mean of values above the 3 rd quartile
skw	Skewness of the histogram of distribution
kurt	Kurtosis of the histogram of the distribution

262 ^{EX}, variables excluded from the analysis.

263 **Multichecks**

264 The second most important part of trident relates to the classification of variables according to
 265 their ability to separate informed categories, such as diet, species, etc. In case study A, the
 266 factor is diet whereas in case study B and C, the factor is species. The software proposes
 267 functions for adding a factor variable by combining variables from different datasets, by
 268 entering it manually or automatically (see Supplementary Materials 2).

269 Afterward, the discriminant ability of variables is calculated using a pipeline of analysis initially
270 designed by Francisco and colleagues (Francisco, Blondel, et al., 2018; Francisco, Brunetière,
271 et al., 2018):

272 (a) Normality: the normality of the data is tested using the Shapiro-Wilk test. If
273 unsuccessful, we compute the skewness ratio, computed as the skewness divided by
274 its confidence interval. If the skewness ratio is inferior to 2, the distribution is
275 considered nearly normal.

276 (b) Homoscedasticity: for normally distributed data, the homogeneity of variances is tested
277 using the Bartlett test. If the test fails, the groups are still nearly homoscedastic if the
278 variance ratio, computed as the maximum variance divided by the minimum variance
279 for each group, is lower than 3. For nearly normal data, Levene's test is performed to
280 check the group variance homogeneity.

281 (c) Ability to separate categories: If both normality and homoscedasticity assumptions are
282 respected, or if no more than one condition is nearly respected, then the discriminant
283 ability of variables is tested using an ANOVA. Otherwise, the discriminant ability of
284 variables is tested using a non-parametric test, the Kruskal-Wallis test.

285 All these tests are implemented with a default alpha of 0.05. They have been grouped in a
286 'multi check' function (Supplementary Materials 2). If data are not normally distributed, they
287 can also be transformed using either a base 10 logarithm function or a Box-Cox
288 transformation (Supplementary Materials 2).

289 ***Classification of variables***

290 We implemented five different classification methods, which can be used depending on the
291 situation:

292 (1) Rank based on ANOVA: Performs an ANOVA and arranges variables by ascending p-
293 value. The purpose here is to separate discriminant from non-discriminant variables. To

294 make things easier for users, variables are ranked by the p values of the ANOVA. One
295 could be interested to have a first glance at the discriminant variables and most
296 discriminating ones whatever the number of groups involved in the study.

297 (2) Rank based on Kruskal-Wallis: Performs a Kruskal-Wallis rank-sum test and arranges
298 variables by ascending p-value; in case the sample is far from normality or in case of
299 small samples. This way of ranking is equivalent to the first mode but adapted for
300 variables whose distribution does not respect conditions required for parametric tests,
301 meaning that variables are ranked by the p values of the Kruskal Wallis analysis.

302 (3) Rank based on post-hoc (average): Performs an ANOVA and arranges by decreasing
303 the number of significant p-values per pair and then ascending mean p-value from
304 post-hoc tests. The mean p-value can be either arithmetic or geometric, and the user
305 can choose to use only significant p-values to calculate it (this is the default option).
306 This mode allows the users to go further in classifying discriminant variables. The aim
307 is to target the variables that discriminate the highest number of groups. Then, among
308 variables discriminating a same number of groups, we ordered them by the increasing
309 values of the mean of the significant p-values of the post hoc tests (here we have
310 chosen the Tukey test). For instance, with 4 discriminant groups among 7, the mean of
311 the 6 p values of the 6 pairs of significantly different samples is computed for each
312 discriminant variable. They are then ordered. One could then run a PCA on trident or
313 export the dataset with only variables showing differences on the six or five pairs.

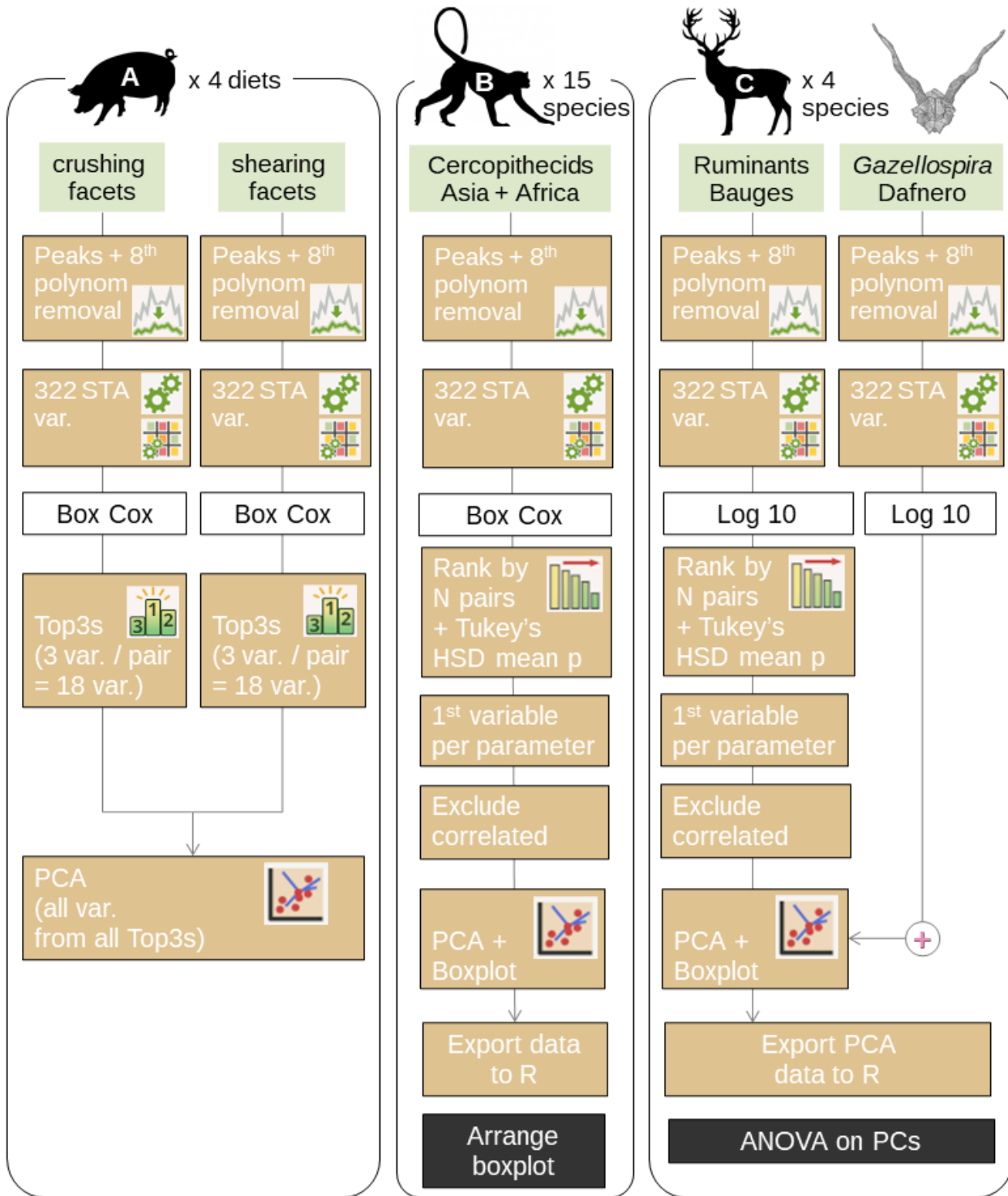
314 (4) Rank based on post-hoc (pairwise): Performs an ANOVA and then for a given pair,
315 arranges variables by ascending pairwise post-hoc p-value. This mode of classification
316 is similar to the former one. However, it differs in targeting variables that discriminate
317 groups of interest. For instance, it can be used for a study including several species for
318 which two of them overlap when considering traditional dental microwear textures

319 although differences were expected because these two species have different feeding
320 preferences. In such a case, trident can select the variables that discriminate the two
321 species at priority.

322 (5) Top 3: For each pair of categories, arranged by the number of significant pairwise p-
323 values from Tukey's HSD, then by the mean of significant p-values. The function
324 returns the 3 best-classified variables. Because this function makes a new
325 classification for each pair of groups, computation time and length of results increase
326 exponentially as the number of categories goes up. Although it remains possible to use
327 this function on any number of categories, we do not recommend using this approach
328 for more than 5 categories (10 pairs). In most cases when comparing a few groups,
329 three parameters appear to be the easiest and fastest way to find out which and how
330 variables discriminate the groups.

331
332 Note that all these tests are implemented with a default alpha of 0.05. Regardless of the
333 chosen workflow, it is possible to visualize variables using boxplots and violin plots. It is also
334 possible to perform a principal component analysis (PCA) on a selection of variables. It
335 provides a histogram of the percentage of variance explained by each principal component
336 (screenplot), as well as buttons for saving and exporting the PCA results, a bivariate diagram
337 of the selected principal components, and circles of correlations. Graphics can be saved as
338 images.

339 **Case-specific analysis**



340

341 Figure 2. Flowchart depicting the analysis for the three case studies; var. = variables; black boxes refer to step
 342 done on R without the use of the graphic interface.

343 ***Case study A: Diet-related differences in dental microwear between controlled-fed pigs.***

344 For each wear facet (crushing and shearing), data were analyzed separately. They were Box-
345 Cox transformed, then checked for normality, homoscedasticity, and their ability to
346 discriminate categories (Fig. 2A). Variables that passed the multi check were classified using
347 the mean of the significant p-values from Tukey's HSD post-hoc analysis of an ANOVA with
348 diet as factor. They were ranked according to (1) the number of groups discriminated and (2)
349 the arithmetic mean of Tukey's HSD discriminant p-values (the p-value of non-discriminated
350 groups were ignored for calculating this arithmetic mean). Among these variables, we retained
351 only the 3 best-ranked variables (Top3). Afterward, all the retained variables for both crushing
352 and shearing facets were combined. We performed a Principal Component Analysis (PCA) to
353 explore their influence on data distribution. All analyses were done exclusively in trident.

354 ***Case study B: Meta-analysis of a large multi-species sample of cercopithecids.***

355 Data were Box-Cox transformed, then checked for normality, homoscedasticity, and their
356 ability to discriminate categories (Fig. 2B). Variables that passed the checking step were
357 classified using the results of a post-hoc analysis of an ANOVA with species as a factor. They
358 were ranked according to (1) the number of groups discriminated and (2) the geometric mean
359 of Tukey's HSD discriminant p-values (the p-value of non-discriminated groups were ignored
360 for calculating this geometric mean). Then, for each parameter (e.g., Asfc2), the best-ranked
361 variable out of 14 (central + heterogeneity statistics, see Table 2) was selected. Afterward, we
362 selected parameters with a correlation of Pearson below 0.70: variables correlated to more
363 than 70 % with a better-ranked variable were systematically removed (calculated
364 independently with R). The remaining variables were used for a PCA. All analyses were done
365 in trident, but the boxplots of the first two principal components were modified for the
366 purposes of this article in R using the ggplot2 package (Wickham et al., 2021).

367 **Case study C: Comparison with extant species to infer the diet of extinct ruminants**

368 First, the Bauges data were log-transformed (base 10), then checked for normality,
369 homoscedasticity and their ability to discriminate species (Fig. 2C). Variables which passed
370 the checking step were classified using (1) the number of groups discriminated by the post-
371 hoc analysis of an ANOVA and (2) the geometric mean of Tukey's HSD discriminant p-values
372 (the p-value of non-discriminated groups were ignored for calculating this geometric mean).
373 Just like case study B, for each parameter (e.g., Asfc2, Sa), the best-ranked variable out of 14
374 (central + heterogeneity statistics) was selected, and variables correlated to more than 70 %
375 with a better-ranked variable were systematically removed (calculated independently with R).
376 The remaining variables were used for a PCA. At this point, the surfaces of *Gazellospira*
377 *torticornis* were added as supplementary individuals to the PCA. All analyses were done in
378 trident, but the boxplots of the first two principal components were modified in R using the
379 ggplot2 package. Afterward, the principal components were exported to R and used for an
380 analysis of variance (ANOVA). The post-hoc analysis was performed using Tukey's HSD test.

381 **Results**

382 **Case study A: Diet-related differences in dental microwear between controlled-fed**
383 **pigs.**

384 The first analysis, a top-3 classification performed on crushing facets after Box-Cox
385 transformation (Table 3), revealed that the most discriminant variables are central height
386 skewness (Ssk), central topology variables (Sk1, Sk2, Smc1, Snb1) and heterogeneity
387 variables for complexity (Asfc2), height (Sq, Sv, Smd) and topology parameters (Sh). In
388 contrast, the same analysis performed on shearing facets (Table 4) revealed that the most
389 discriminating variables are central height kurtosis (Sku), the standard deviation of central
390 height skewness (Ssk.sd), mean and median of Smd, as well as skewness and kurtosis of
391 spatial variables (Sal, r.sl). There are no common variables between the top 3 of crushing and
392 shearing facets.

393 When combining the most discriminating variables from both crushing and shearing facets in
394 a principal component analysis (Fig. 3), the first and second PCs explain 38.2 % and 21.1 %
395 of the variances, respectively. Along PC1 and PC2, the control category overlaps with corn
396 kernels and corn silage categories, but other groups are distinctly separated (Fig. 3A). In fact,
397 PC1 separates barley-fed pigs from other categories, whereas PC2 separates seed-fed pigs
398 (barley and corn) from silage-fed pigs. Other PCs failed to separate categories and were not
399 pictured, but are available as supplementary materials (Supplementary Materials 1).

400 Table 3. Case study A: Diet-related differences in dental microwear on crushing molars facets between
 401 controlled-fed pigs, pairwise top 3 variables for each pair of compared groups ranked by the post hoc p values.
 402 All variables were box-Cox transformed. Ba, barley; Co, control; CK, corn kernel; CS, corn silage (see Figure 2
 403 and method section).

pair i	TOP3 variables for the pair i	rank	F	p value ANOVA	Post hoc p values
Ba-Co	Snb1	1	9.02	<0.01	0.09
	Asfc2.fst.25	2	5.58	0.02	0.09
	Sh.min.05	3	3.69	0.06	0.10
Ba-CK	Sv.lst.25	1	4.47	0.03	0.03
	Sv.max.25	2	4.83	0.03	0.04
	Smc1	3	6.88	0.01	0.04
Ba-CS	Snb1	1	9.02	<0.01	0.02
	Sk1	2	8.33	0.01	0.07
	Asfc2.min.25	3	4.69	0.03	0.07
Co-CK	Smd.kurt	1	4.82	0.03	0.26
	Sk2	2	4.58	0.04	0.39
	Ssk	3	5.45	0.02	0.57
Co-CS	Ssk	1	5.45	0.02	0.15
	Sq.kurt	2	5.21	0.03	0.45
	Smd.kurt	3	4.82	0.03	0.54
CK-CS	Smd.kurt	1	4.82	0.03	0.02
	Sq.kurt	2	5.21	0.03	0.07
	Sk2	3	4.58	0.04	0.35

404 Table 4. Case study A: Diet-related differences in dental microwear between controlled-fed pigs, pairwise top 3
 405 variables for the shearing facets. All variables Box-Cox transformed. Ba, barley; Co, control; CK, corn kernel; CS,
 406 corn silage (see Figure 2 and method section).

pair <i>i</i>	TOP3 variables for the pair <i>i</i>	rank	<i>F</i>	<i>p</i> value ANOVA	Post hoc <i>p</i> values
Ba-Co	Sal.kurt	1	3.68	0.06	0.01
	r.sl.skew	2	5.49	0.02	0.28
	Smd.mean	3	5.18	0.03	0.28
Ba-CK	Smd.mean	1	5.18	0.03	0.05
	Sal.kurt	2	3.68	0.06	0.06
	Smd.median	3	5.76	0.02	0.07
Ba-CS	r.sl.kurt	1	5.68	0.02	0.11
	Sku	2	3.85	0.05	0.13
	r.sl.skew	3	5.49	0.02	0.17
Co-CK	r.sl.skew	1	5.49	0.02	0.12
	r.sl.kurt	2	5.68	0.02	0.13
	Ssk.sd	3	6.01	0.02	0.62
Co-CS	Sku	1	3.85	0.05	0.03
	Sal.kurt	2	3.68	0.06	0.24
	Ssk.sd	3	6.01	0.02	0.36
CK-CS	Sku	1	3.85	0.05	0.02
	r.sl.kurt	2	5.68	0.02	0.03
	Ssk.sd	3	6.01	0.02	0.04

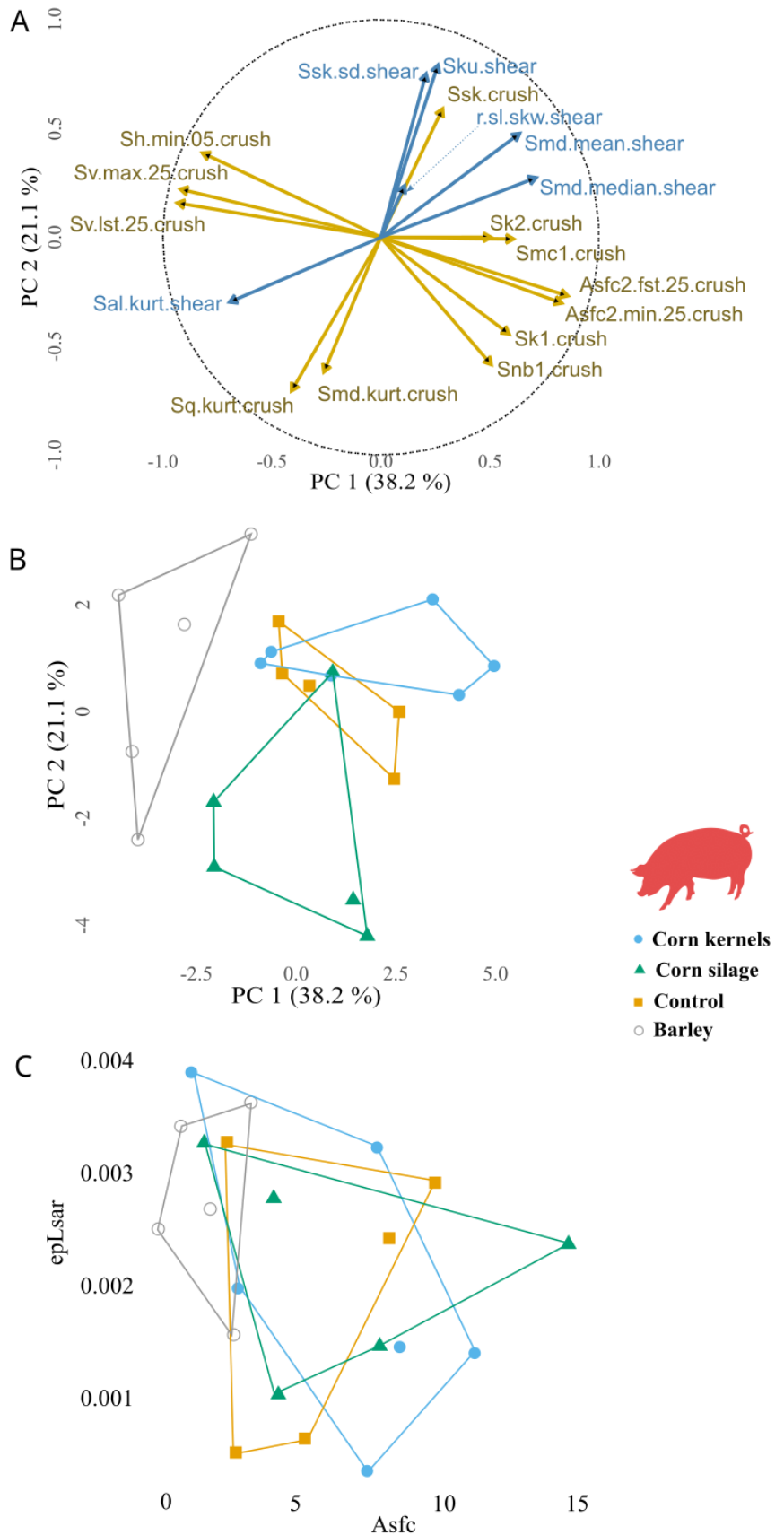
407

408

409

410
 411
 412
 413
 414
 415
 416
 417
 418
 419
 420
 421
 422
 423
 424
 425

Figure 3. Case study A: Diet-related differences in dental microwear between controlled-fed pigs, from crushing and shearing facets of upper deciduous fourth premolar. Principal component analysis from the top 3 variables for each pair of dietary categories (A & B) compared with the classical SSFA biplots. A, correlation circle, PC1 versus PC2; B, bivariate graph of individuals along PC1 versus PC2; C, bivariate graph of individuals with SSFA parameters Asfc and epLsar.



426 **Case study B: Meta-analysis of a large multi-species sample of cercopithecids.**

427 The analysis, a rank by post-hoc (mean) classification performed on crushing facets after
428 Box-Cox transformation (Table 5), revealed that the most discriminant variables were a mix of
429 central and heterogeneity variables. After removing variables correlated with the best ranked
430 variables, the majority of variables are heterogeneity variables related to the highest
431 percentiles among subsampled tiles (Sh.lst.05, Asfc2.max.05, Smc2.lst.25, s.sl.lst.05,
432 b.sl.max.05 and Sku.lst.25).

433 The major influence of the highest percentile variables is confirmed by the PCA (Fig. 4).
434 Indeed, these variables contribute significantly to the first and second components, which
435 explain 42.8 % and 22.6 % of the variance, respectively (Fig. 4B). This is also consistent with
436 the difference in absolute surface height, which is clear on the maps: along the first
437 component, the highest value has a height amplitude of 10.95 μm (Fig. 4C, 4D) while the
438 lowest value has a height amplitude of 0.71 μm (Fig. 4C, 4E).

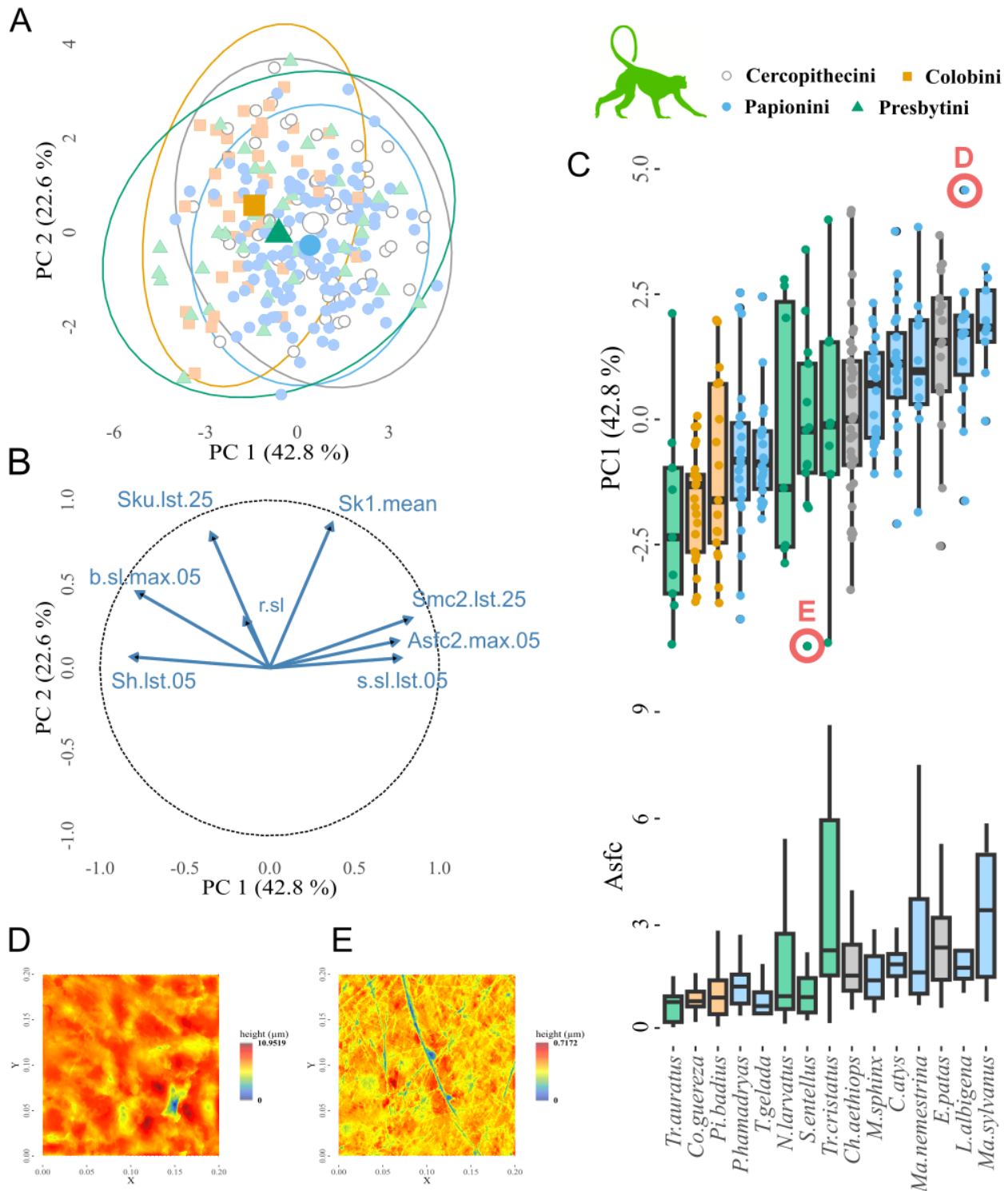
439 The bivariate graph of individuals for components 1 and 2, as well as the boxplot of
440 component 1, show that there is a large overlap between categories, both at the species and
441 the tribe level (Fig. 4A, 4C). This is due to the broad dispersion of values. When comparing
442 the means between species (Fig. 4C), the most folivorous species (*Trachypithecus auratus*,
443 *Colobus guereza* and *Ptilocolobus badius*) have the lowest PC1 values. They are followed by
444 terrestrial graminivorous papionines *Papio hamadryas* and *Theropithecus gelada*, then
445 *Nasalis larvatus*, *Semnopithecus entellus* and *Trachypithecus cristatus*. The latter three are
446 also folivorous but present higher Asfc2 values in our sample, indicating the opportunistic
447 consumption of seeds (Thiery et al., 2021). This is supported by the surprisingly large breadth
448 of PC1 value dispersion for these three species, especially *T. cristatus*. Then, opportunistic
449 terrestrial cercopithecines and papionines show higher PC1 values, with the highest values

450 found in the hard seed predator *Lophocebus albigena* (Lambert et al., 2004) and *Macaca*
451 *sylvanus*, one of the most granivorous macaque (Kato et al., 2014).

452 Table 5. Case study B; Meta-analysis of a large multi-species sample of cercopithecids, the most discriminant
 453 variables for each family, classified by the number of pair (N) that shows significant differences with the Tukey's
 454 HSD p-value.

Variable	Position	ANOVA			Tukey's HSD	
		F	p value	mean p-value	geometric mean p-value	N (among 105 pairs)
Sh.lst.05	1	11.29	<0.01	0.01	<0.01	37
Asfc2.max.05	5	7.62	<0.01	0.01	<0.01	32
Sp.max.25	12	9.48	<0.01	0.01	0.01	24
Sa	13	9.39	<0.01	0.01	<0.01	23
Sq	15	9.03	<0.01	0.01	0.01	23
Sv.fst.05	16	6.11	<0.01	0.01	0.01	23
Sdar.max.05	18	6.37	<0.01	0.01	<0.01	22
Smd.max.25	25	5.84	<0.01	0.01	<0.01	17
Smc2.lst.25	29	6.58	<0.01	0.01	<0.01	15
Smc1.min.25	30	5.73	<0.01	0.02	<0.01	15
Sk2.mean	33	4.51	<0.01	0.02	0.01	15
Sm.min.25	36	6.41	<0.01	0.02	0.01	14
s.sl.lst.05	45	4.71	<0.01	0.02	0.02	13
b.sl.max.05	49	6.37	<0.01	0.01	<0.01	12
Snb2.mean	60	3.53	<0.01	0.02	0.01	12
Sal.min.05	73	5.85	<0.01	0.01	<0.01	10
Sku.lst.25	83	3.42	<0.01	0.01	<0.01	9
Sk1.mean	92	4.72	<0.01	0.03	0.02	9
r.sl	99	4.88	<0.01	0.01	<0.01	7
Stri	101	4.89	<0.01	0.01	<0.01	7
Ssk.fst.05	103	4.08	<0.01	0.02	0.01	7
Snb1.sd	149	3.30	<0.01	0.02	0.01	4

455 All variables Box-Cox transformed. For each parameter (e.g., Sh), only the variable with the best positioning
 456 was selected (e.g., Sh.lst.05). Highlighted in grey are the best-positioned variables which are little correlated to
 457 each other (threshold: 0.7).
 458



459
 460 Figure 4. Case study B: Meta-analysis of a large multi-species sample of cercopithecids. Analysis of dental
 461 microwear textures from the crushing facets of upper and lower molars of cercopithecids from Asia and Africa.
 462 Principal component analysis was performed using the best-ranked non-correlated variables. A, bivariate graph
 463 of individuals along PC1 versus PC2 with ellipses depicting the confidence interval at 95 %; B, correlation circle,
 464 PC1 versus PC2; C, Boxplot of PC1 values, ordered by ascending mean, with species as a factor compared with
 465 boxplots of Asfc values (individuals are not shown to make the figure easier to read.; D, height map of the
 466 surface from the individual with the highest PC1 value (*L. albigena*_NHMB-LP-2908); E, height map of the
 467 surface from the individual with the lowest PC1 value (*S. entellus*_BM30-11-1-4).

468 **Case study C: Comparison with extant species to infer the diet of extinct ruminants**

469 The first part of the analysis, a rank by post-hoc (mean) classification performed, after a base-
470 10 log transformation, on the shearing dental facets of molars of the wild-caught ruminants
471 from the Bauges Natural Regional Park (Table 6), revealed once again that most discriminant
472 variables were a mix of central and heterogeneity variables. After removing variables
473 correlated with the best-ranked variables, what remains are variables based on spatial
474 parameters (Rmax.min.25, s.sl.mean, r.sl), the standard deviation of topology parameters
475 (Sk1.sd, Smc1.sd) and Sm.fst.25, which is the first quartile of the lowest parts of the surface's
476 height.

477 The first two dimensions of the PCA encompass 43.9 % and 27.6 % of the variance,
478 respectively. On the first dimension, we found that *G. torticornis* significantly differed from both
479 *C. capreolus* and *C. elaphus* (Table 7). In contrast, there was no significant difference
480 between *G. torticornis*, *R. rupicapra* and *O. gmelini*, which is visible on the bivariate graph and
481 on the boxplot (Fig. 5C, D). On the second dimension as well on the third and fourth
482 dimensions, *G. torticornis* was significantly different from all extant species whereas no
483 difference could be detected between extant species. Overall, *G. torticornis* had on average
484 lower values than extant species for both the first and second dimensions (Fig. 5D, E).

485

486

487 Table 6. Case study C: Comparison with extant species to infer the diet of extinct ruminants, the most
 488 discriminant variables for each parameter, classified by the number of pair (N) that shows significant differences
 489 with the Tukey's HSD p-value.
 490

Variable	rank	F	p value			N (among 6 pairs)
			ANOVA	HSD _{arithmetic mean}	HSD _{geometric mean}	
Rmax.min.25	1	7.93	<0.01	0.02	0.01	4
Snb1.sd	2	9.19	<0.01	0.01	<0.01	3
Sku.lst.25	12	6.38	<0.01	0.01	<0.01	2
Sk1.sd	13	4.38	0.01	0.01	0.01	2
Ssk.max.05	14	5.08	<0.01	0.02	0.01	2
b.sl.min.25	21	5.10	<0.01	0.02	0.01	2
Sm.fst.25	27	3.65	0.02	0.03	0.02	2
s.sl.mean	30	5.49	<0.01	0.03	0.03	2
Smd.min.05	32	3.36	0.03	0.03	0.03	2
Smc1.sd	36	4.27	0.01	0.03	0.03	2
Snb2.sd	49	5.22	<0.01	<0.01	<0.01	1
Sal	55	4.26	0.01	0.02	0.02	1
r.sl	63	3.00	0.04	0.03	0.03	1
Sa.lst.25	70	3.45	0.02	0.04	0.04	1
Stri	72	2.27	0.09	0.04	0.04	1

491 All data log-transformed (base 10). For each parameter (e.g., Rmax), only the variable with the best positioning
 492 was selected (e.g., Rmax.min.25). Highlighted in grey are the best positioned variables which are little correlated
 493 to each others (threshold: 0.7).
 494

495

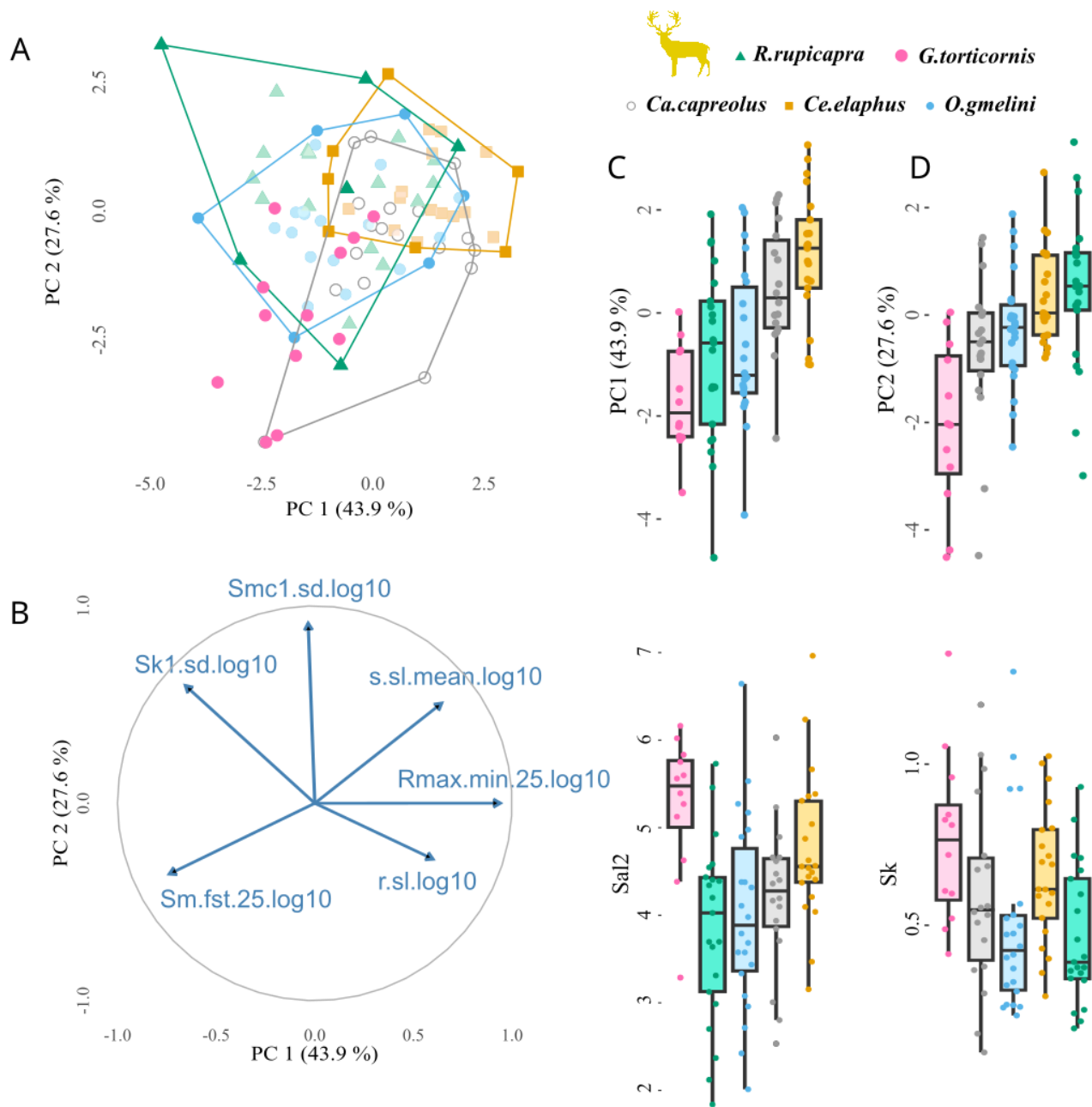
496

497

498 Table 7. Case study C: Comparison between extant and extinct species to infer the diet of the extinct ruminants
 499 thanks to ANOVA on the first four principal components and followed by pairwise comparison of the means using
 500 Tukey's HSD.

Pair	PC1 (43.9 %)		PC2 (27.6 %)		PC3 (14.6 %)		PC4 (7.9 %)	
	Difference	p adjusted	Difference	p adjusted	Difference	p adjusted	Difference	p adjusted
CE-CC	0.61	0.66	1.02	0.10	-0.01	1.00	0.15	0.97
OG-CC	-1.14	0.09	0.39	0.87	-0.40	0.64	0.06	1.00
RR-CC	-1.31	0.04	1.12	0.06	0.28	0.87	0.15	0.96
OG-CE	-1.75	<0.01	-0.63	0.50	-0.39	0.63	-0.09	0.99
RR-CE	-1.92	<0.01	0.10	1.00	0.29	0.84	0.00	1.00
RR-OG	-0.17	0.99	0.73	0.34	0.68	0.11	0.09	0.99
GT-CC	-2.17	<0.01	-1.39	0.03	-1.54	<0.01	-1.97	<0.01
GT-CE	-2.78	<0.01	-2.41	<0.01	-1.53	<0.01	-2.12	<0.01
GT-OG	1.03	0.25	1.79	<0.01	1.14	0.01	2.03	<0.01
GT-RR	0.86	0.44	2.52	<0.01	1.82	<0.01	2.12	<0.01

501 Highlighted in grey are the differences supported by a significant adjusted p value. CE, *Cervus elaphus*; CC,
 502 *Capreolus capreolus*; GT, *Gazellospira torticornis*; OG, *Ovis gmelini*; RR, *Rupicapra rupicapra*.
 503



504
 505 Figure 5. Case study C: Comparison with extant species to infer the diet of extinct species of ruminants, PCA on
 506 selected variables with ruminants from the Bauges as individuals and fossil specimens of *Gazellospira torticornis*
 507 as supplementary individuals. A, Bivariate graph of individuals along PC1 versus PC2, with the extinct species
 508 from Dafnero *Gazellospira torticornis* as supplementary individuals (pink); B, Correlation circle, PC1 versus PC2;
 509 C, Boxplot of PC1 values, ordered by ascending mean, with species as a factor in comparison with texture
 510 spatial parameters (Sal2; Sal calculated with $s = 0.5$) ; D, Boxplot of PC2 values, ordered by ascending mean,
 511 with species as a factor in comparison with the Sk parameter related to vertical material distribution. All data log-
 512 transformed (base 10).

513 **Discussion**

514 **Case study A: Diet-related differences in dental microwear between controlled-fed** 515 **pigs**

516 The broad spectrum of analytic tools and exploratory methods offered by trident maximizes
517 the potential for detecting diet-related differences in dental microwear. In case study A, the
518 four groups could be separated, which is consistent with Louail et al. (2021), but the
519 difference between categories was enhanced. Dental microwear sometimes shows large
520 within-species differences, including in wild animals (Calandra & Merceron, 2016, Percher et
521 al., 2018) and extinct species (Scott et al., 2005; Thiery et al., 2021). In our case study
522 however, even the subtlest variations in diet, for instance between the corn silage and the
523 control groups, could be detected. These results are promising for paleontological and
524 archaeological studies interested in diet variation across time and space.

525 In addition, trident is also compatible with other workflows, as it can easily combine multiple
526 datasets, for instance microwear measured using different methods (SSFA, light
527 microscopy...), from different teeth, or different parts of a tooth – as in case study A. In this
528 case study, we found that shearing and crushing facets not only differ in microwear textures
529 but also in the best-ranked variables diet-wise. Crushing different kinds of food influenced the
530 skewness and heterogeneity of microwear height, whereas shearing different kinds of foods
531 had a more visible influence on height kurtosis, on standard deviation of height skewness, on
532 median height, as well as skewness and kurtosis of spatial parameters. For crushing, the
533 presence of large and deep pits resulting from the processing of hard, seed-like foods is
534 indeed expected to affect height and its heterogeneity. For shearing on the other hand, spatial
535 parameters, and especially anisotropy, are expected to be more affected by the long shearing
536 motions of tough, high-energy release rate foods such as leaves, grass etc. This is consistent

537 with our results, and demonstrates that trident can not only integrate multiple methods, but
538 also leverage their input.

539 **Case study B: Meta-analysis of a large multi-species sample of cercopithecids**

540 Sometimes the objective is not to separate groups of individuals but to identify patterns of
541 variation imputable to dietary trends. This is exactly what trident enabled in case study B:
542 despite PC1 values overlapping between cercopithecoid species, we can distinguish a
543 continuum from strict leaf consumption to staple seed predation (Fig. 4). The most folivorous
544 species (*Trachypithecus auratus*, *Colobus guereza* and *Ptilocolobus badius*) have the lowest
545 PC1 values, whereas opportunistic terrestrial cercopithecines and papionines show higher
546 PC1 values, with the highest values found in *Lophocebus albigena* and *Macaca sylvanus*, two
547 notable seed eaters (Lambert et al., 2004; Kato et al., 2014). Detecting this pattern required
548 trident for ranking variables by mean p-value of Tukey's HSD and for performing multivariate
549 analysis on the best non-correlated variables, but also the R environment for ordering
550 species-related boxplots by ascending mean (Fig. 4C). It shows the interest of nesting trident
551 within the R environment: accessing a broad range of libraries for complementing and
552 leveraging functions from the R package trident.

553 The trident package in R (but not the graphic interface) also allows to inspect surfaces using
554 2D and 3D maps – although these functions are not implemented into the interface, they can
555 be launched from R (see Supplementary Materials 2). Here, the highest PC1 values are
556 characterized by high maximal complexity, but also deeply worn surfaces (Fig. 4D). In
557 contrast, the lowest PC1 values are characterized by a low complexity and shallow wear
558 marks (Fig. 4E). Both a higher complexity (Ramdarshan et al., 2016) and larger, deeper pits
559 (Teaford, 1985, 1988) have been associated to the ingestion of large amounts of seed kernels,
560 which is consistent with the pattern observed on Fig. 4C. It is also consistent with Asfc2

561 successfully separating seed-eating cercopithecids in previous studies (e.g., Thiery et al.,
562 2021). In short, trident helps detect patterns in dental microwear textures, but it also and
563 foremost helps interpret them in biomechanical or ecological terms.

564 **Case study C: Comparison with extant species to infer the diet of extinct ruminants**

565 The last key use of trident is the inference of diet, either in extant or in extinct species. In case
566 study C, we could infer the diet of *Gazellospira torticornis*, an extinct antelope from the Early
567 Pleistocene of Greece (Hermier *et al.*, 2020). To do so, we used trident to perform a PCA on
568 the best ranked, non-correlated variables regarding their ability to separate four ruminants
569 from the Bauges Natural Regional Park with known differences in diet, ranging from selective
570 browsing to grass-dominated mixed feeding habits. We then added *G. torticornis* specimens
571 as supplementary individuals to the PCA. This analysis showed that *G. torticornis* had low
572 values of anisotropy, especially the 1st quartile (Rmax.min.25, Fig. 5), which is similar to *Ovis*
573 *gmelini* and *Rupicapra rupicapra*. Both are mixed-feeding species: *O. gmelini musimon* eats
574 grasses in complement with dicots foliages, shrubs and herbaceous dicots (Redjadj et al.
575 2014; see also Marchand et al., 2013), while *R. rupicapra* alternates between grass and
576 foliage depending on seasons (Redjadj et al. 2014; see also Pérez-Barberia et al., 1997). *G.*
577 *torticornis* likely was a mixed feeding species, incorporating both grasses and lignified tissues
578 in its diet.

579 Once again, nesting trident in the R environment gives access to a broad range of methods
580 for complementary analysis. To better understand the dietary behavior of *G. torticornis*, we
581 performed an ANOVA on principal components to search for differences between extinct and
582 extant taxa. For PC1, *G. torticornis* significantly differed from *Cervus elaphus* and *Capreolus*
583 *capreolus*. *C. elaphus* is also a mixed-feeding species (Gebert & Verheyden-Tixier, 2001), but
584 in the Bauges Natural Regional Park, its diet comprises a large proportion of grasses

585 (Merceron et al., 2021a). This likely increased its dental microwear anisotropy, which explains
586 why it differs from other mixed-feeders that include more lignified tissues than the red deer. *C.*
587 *capreolus* on the other hand is a selective browser (Redjadj et al., 2014).
588 Lastly, variables that contribute to PC2 (Smc1.sd and to some extent, Sk1.sd and s.sl.mean)
589 were significantly lower in *G. torticornis* compared to all four extant species. This point
590 illustrates how dental microwear textures can present original patterns in the fossil record,
591 sometimes completely different to what is known for extant species – perhaps reflecting how
592 different the environmental conditions were at the time.

593 **Conclusion**

594 trident, an R package for performing dental microwear texture analysis is here proposed and
595 shown with three case studies, showing how trident helps answer questions commonly
596 investigated by paleontologists and archaeologists. In the first case study, we separate four
597 groups of domestic pigs based on their dietary composition. In the second case study, we
598 identify microwear texture patterns in a large database of 15 primate species and relate these
599 patterns to biomechanical and ecological factors. The third case study investigates the dental
600 microwear textures of four extant ruminants to infer the diet of an extinct antelope from the
601 Pleistocene of Greece. These case studies show how trident can leverage dental microwear
602 texture analysis results.

603 **Acknowledgments**

604 This study was funded by the French National Agency for Research (ANR-13-JSV7-0008-01
605 Trident, PI: Gildas Merceron; ANR-17-CE27-0002-02 DIET-Scratches, PIs: Gildas Merceron,
606 Stéphane Ferchaud) and the Region of Nouvelle Aquitaine (ALIHOM #210389; PI: Gildas
607 Merceron). We thank all the people, and especially Anusha Ramdarshan, Antoine Souron and
608 Franck Guy, who improved trident during its development,. Our gratitude also goes towards

609 the colleagues who allowed or participated in data collection for the three case studies,
610 notably Jérôme Surault (PALEVOPRIM). Finally, we thank the reviewers and the
611 recommender for their constructive comments and suggestions.

612 **Authors' contributions**

613 AF, NB, and GM conceived the ideas and designed the methodology; GM, EB, CB, ML, and
614 AW collected the data; AF, GM, ML, and GT developed the software; AF and GT coded the
615 software program; ML, GM and GT analysed the data; GM acquired funding and managed
616 the project administration. All authors contributed critically to the drafts and gave final
617 approval for publication.

618 **Data availability**

619 The source package is available on Github at <https://github.com/nialsiG/trident>.

620 Dental Microwear Texture are available in the repository InDores. All raw scans of surfaces
621 (plu ou plux files), the template used to pre-treat raw data (mnt files), as well as the surfaces
622 (.sur files) used with trident are provided here

623 **Conflict of interest disclosure**

624 The authors of this preprint declare that they have no financial conflict of interest with the
625 content of this article.

626

627 **References**

628

- Calandra, I., & Merceron, G. (2016). Dental microwear texture analysis in mammalian ecology: DMTA in ecology. *Mammal Review*, *46*(3), 215–228. <https://doi.org/10.1111/mam.12063>
- Clauss, M., Fritz, J., & Hummel, J. (2023). Teeth and the gastrointestinal tract in mammals: when 1+ 1= 3. *Philosophical Transactions of the Royal Society B*, *378*(1891), 20220544.
- Francisco, A., Blondel, C., Brunetière, N., Ramdarshan, A., & Merceron, G. (2018a). Enamel surface topography analysis for diet discrimination. A methodology to enhance and select discriminative parameters. *Surface Topography: Metrology and Properties*, *6*(1), 015002. <https://doi.org/10.1088/2051-672X/aa9dd3>
- Francisco, A., Brunetière, N., & Merceron, G. (2018b). Gathering and Analyzing Surface Parameters for Diet Identification Purposes. *Technologies*, *6*(3), 75. <https://doi.org/10.3390/technologies6030075>
- Galbany, J., Martínez, L. M., López-Amor, H. M., Espurz, V., Hiraldo, O., Romero, A., de Juan, J., & Pérez-Pérez, A. (2005). Error rates in buccal-dental microwear quantification using scanning electron microscopy. *Scanning*, *27*(1), 23–29. <https://doi.org/10.1002/sca.4950270105>
- Gebert, C., & Verheyden-Tixier, H. (2001). Variations of diet composition of Red Deer (*Cervus elaphus* L.) in Europe. *Mammal Review*, *31*(3–4), 189–201. <https://doi.org/10.1111/j.1365-2907.2001.00090.x>
- Gordon, K. D. (1982). A study of microwear on chimpanzee molars: Implications for dental microwear analysis. *American Journal of Physical Anthropology*, *59*(2), 195–215. <https://doi.org/10.1002/ajpa.1330590208>
- Grine, F. E., Ungar, P. S., & Teaford, M. F. (2002). Error rates in dental microwear quantification using scanning electron microscopy. *Scanning*, *24*(3), 144–153. <https://doi.org/10.1002/sca.4950240307>
- Hermier, R., Merceron, G., & Kostopoulos, D. S. (2020). The emblematic Eurasian Villafranchian antelope *Gazellospira* (Mammalia: Bovidae): New insights from the Lower Pleistocene Dafnero fossil sites (Northern Greece). *Geobios*, *61*, 11–29.

- Hua, L., Chen, J., & Ungar, P. S. (2020). Diet reduces the effect of exogenous grit on tooth microwear. *Biosurface and Biotribology*, 6(2), 48–52. <https://doi.org/10.1049/bsbt.2019.0041>
- Kaiser, T. M., Clauss, M., & Schulz-Kornas, E. (2015). A set of hypotheses on tribology of mammalian herbivore teeth. *Surface Topography: Metrology and Properties*, 4(1), 014003. <https://doi.org/10.1088/2051-672X/4/1/014003>
- Kato, A., Tang, N., Borries, C., Papakyrikos, A. M., Hinde, K., Miller, E., Kunimatsu, Y., Hirasaki, E., Shimizu, D., & Smith, T. M. (2014). Intra- and interspecific variation in macaque molar enamel thickness. *American Journal of Physical Anthropology*, 155(3), 447–459. <https://doi.org/10.1002/ajpa.22593>
- Kay, R. F. (1981). The ontogeny of premolar dental wear in *Cercocebus albigena* (cercopithecidae). *American Journal of Physical Anthropology*, 54(1), 153–155. <https://doi.org/10.1002/ajpa.1330540119>
- Kubo, M. O., & Fujita, M. (2021). Diets of Pleistocene insular dwarf deer revealed by dental microwear texture analysis. *Palaeogeography, Palaeoclimatology, Palaeoecology*, 562, 110098.
- Lambert, J. E., Chapman, C. A., Wrangham, R. W., & Conklin-Brittain, N. L. (2004). Hardness of cercopithecine foods: Implications for the critical function of enamel thickness in exploiting fallback foods. *American Journal of Physical Anthropology*, 125(4), 363–368. <https://doi.org/10.1002/ajpa.10403>
- Louail, M., Ferchaud, S., Souron, A., Walker, A. E. C., & Merceron, G. (2021). Dental microwear textures differ in pigs with overall similar diets but fed with different seeds. *Palaeogeography, Palaeoclimatology, Palaeoecology*, 572, 110415. <https://doi.org/10.1016/j.palaeo.2021.110415>
- Lucas, P. W., Omar, R., Al-Fadhlah, K., Almusallam, A. S., Henry, A. G., Michael, S., Thai, L. A., Watzke, J., Strait, D. S., & Atkins, A. G. (2013). Mechanisms and causes of wear in tooth enamel: Implications for hominin diets. *Journal of The Royal Society Interface*, 10(80), 20120923. <https://doi.org/10.1098/rsif.2012.0923>
- Marchand, P., Redjadj, C., Garel, M., Cugnasse, J.-M., Maillard, D., & Loison, A. (2013). Are mouflon *Ovis gmelini musimon* really grazers? A review of variation in diet composition. *Mammal Review*, 43(4), 275–291. <https://doi.org/10.1111/mam.12000>

- Merceron, G., Berlioz, E., Vohnhof, H., Green, D., Garel, M., & Tütken, T. (2021a). Tooth tales told by dental diet proxies: An alpine community of sympatric ruminants as a model to decipher the ecology of fossil fauna. *Palaeogeography, Palaeoclimatology, Palaeoecology*, 562, 110077.
- Merceron, G., Blondel, C., Bonis, L. D., Koufos, G. D., & Viriot, L. (2005). A New Method of Dental Microwear Analysis: Application to Extant Primates and *Ouranopithecus macedoniensis* (Late Miocene of Greece). *PALAIOS*, 20(6), 551–561. <https://doi.org/10.2110/palo.2004.p04-17>
- Merceron, G., Bonis, L., Viriot, L., & Blondel, C. (2005). Dental microwear of the late Miocene bovids of northern Greece: Vallesian/Turolian environmental changes and disappearance of *Ouranopithecus macedoniensis*? *Bulletin de La Societe Geologique de France*, 176, 475–484. <https://doi.org/10.2113/176.5.475>
- Merceron, G., Kallend, A., Francisco, A., Louail, M., Martin, F., Plastiras, C.-A., Thiery, G., & Boisserie, J.-R. (2021b). Further away with dental microwear analysis: Food resource partitioning among Plio-Pleistocene monkeys from the Shungura Formation, Ethiopia. *Palaeogeography, Palaeoclimatology, Palaeoecology*, 572, 110414. <https://doi.org/10.1016/j.palaeo.2021.110414>
- Merceron, G., Ramdarshan, A., Blondel, C., Boisserie, J.-R., Brunetiere, N., Francisco, A., Gautier, D., Milhet, X., Novello, A., & Pret, D. (2016). Untangling the environmental from the dietary: Dust does not matter. *Proceedings of the Royal Society B: Biological Sciences*, 283(1838), 20161032. <https://doi.org/10.1098/rspb.2016.1032>
- Mihlbachler, M. C., Beatty, B. L., Caldera-Siu, A., Chan, D., & Lee, R. (2012). Error rates and observer bias in dental microwear analysis using light microscopy. *Palaeontologia Electronica*, 15(1), 1–22. <https://doi.org/10.26879/298>
- Percher, A.M., Merceron, G., Nsi Akoue, G., Galbany, J., Romero, A., & Charpentier, M.J. (2018). Dental microwear textural analysis as an analytical tool to depict individual traits and reconstruct the diet of a primate. *American Journal of Physical Anthropology*, 165, 123–138. <https://doi.org/10.1002/ajpa.23337>
- Peréz-Barberia, F. J., Oliván, M., Osoro, K., & Nores, C. (1997). Sex, seasonal and spatial differences in the diet of Cantabrian chamois *Rupicapra pyrenaica parva*. *Acta Theriologica*, 42(1), 37–46.

- Purnell, M. A., Crumpton, N., Gill, P. G., Jones, G., & Rayfield, E. J. (2013). Within-guild dietary discrimination from 3-D textural analysis of tooth microwear in insectivorous mammals. *Journal of Zoology*, 291(4), 249–257. <https://doi.org/10.1111/jzo.12068>
- Ramdarshan, A., Blondel, C., Brunetière, N., Francisco, A., Gautier, D., Surault, J., & Merceron, G. (2016). Seeds, browse, and tooth wear: A sheep perspective. *Ecology and Evolution*, 6(16), 5559–5569. <https://doi.org/10.1002/ece3.2241>
- Redjadj, C., Darmon, G., Maillard, D., Chevrier, T., Bastianelli, D., Verheyden, H., Loison, A., & Saïd, S. (2014). Intra- and Interspecific Differences in Diet Quality and Composition in a Large Herbivore Community. *PLOS ONE*, 9(2), e84756. <https://doi.org/10.1371/journal.pone.0084756>
- Rivals, F., & Semprebon, G. M. (2011). Dietary plasticity in ungulates: insight from tooth microwear analysis. *Quaternary International*, 245(2), 279–284. <https://doi:10.1016/j.quaint.2010.08.001>
- Rowe, N., Goodall, J., & Mittermeier, R. (1996). *The pictorial guide to the living primates* (Vol. 236). Pogonias Press.
- Sakaki, H., Winkler, D. E., Kubo, T., Hirayama, R., Uno, H., Miyata, S., Endo, H., Sasaki, K., Takisawa, T., & Kubo, M. O. (2022). Non-occlusal dental microwear texture analysis of a titanosauriform sauropod dinosaur from the Upper Cretaceous (Turonian) Tamagawa Formation, northeastern Japan. *Cretaceous Research*, 136, 105218.
- Sanson, G. D., Kerr, S. A., & Gross, K. A. (2007). Do silica phytoliths really wear mammalian teeth? *Journal of Archaeological Science*, 34(4), 526–531. <https://doi.org/10.1016/j.jas.2006.06.009>
- Schulz, E., Calandra, I., & Kaiser, T. M. (2010). Applying tribology to teeth of hoofed mammals. *Scanning*, 32(4), 162–182. <https://doi.org/10.1002/sca.20181>
- Schulz- Kornas, E., Stuhlträger, J., Clauss, M., Wittig, R. M., & Kupczik, K. (2019). Dust affects chewing efficiency and tooth wear in forest dwelling Western chimpanzees (*Pan troglodytes verus*). *American Journal of Physical Anthropology*, 169(1), 66–77. <https://doi.org/10.1002/ajpa.23808>
- Schulz-Kornas, E., Winkler, D. E., Clauss, M., Carlsson, J., Ackermans, N. L., Martin, L. F., Hummel, J., Müller, D. W. H., Hatt, J.-M., & Kaiser, T. M. (2020). Everything matters: Molar microwear

- texture in goats (*Capra aegagrus hircus*) fed diets of different abrasiveness. *Palaeogeography, Palaeoclimatology, Palaeoecology*, 552, 109783. <https://doi.org/10.1016/j.palaeo.2020.109783>
- Scott, R. S., Ungar, P. S., Bergstrom, T. S., Brown, C. A., Childs, B. E., Teaford, M. F., & Walker, A. (2006). Dental microwear texture analysis: Technical considerations. *Journal of Human Evolution*, 51(4), 339–349. <https://doi.org/10.1016/j.jhevol.2006.04.006>
- Scott, R. S., Ungar, P. S., Bergstrom, T. S., Brown, C. A., Grine, F. E., Teaford, M. F., & Walker, A. (2005). Dental microwear texture analysis shows within-species diet variability in fossil hominins. *Nature*, 436(7051), 693–695. <https://doi.org/10.1038/nature03822>
- Solounias, N., & Semperebon, G. (2002). Advances in the reconstruction of ungulate ecomorphology with application to early fossil equids. *American Museum Novitates*, 2002(3366), 1-49. [https://doi.org/10.1206/0003-0082\(2002\)366<0001:AITROU>2.0.CO;2](https://doi.org/10.1206/0003-0082(2002)366<0001:AITROU>2.0.CO;2)
- Teaford, M. F. (1985). Molar microwear and diet in the genus *Cebus*. *American Journal of Physical Anthropology*, 66(4), 363–370. <https://doi.org/10.1002/ajpa.1330660403>
- Teaford, M. F. (1988). A review of dental microwear and diet in modern mammals. *Scanning Microscopy*, 2(2), 1149–1166.
- Teaford, M. F., Maas, M. C., & Simons, E. L. (1996). Dental microwear and microstructure in early oligocene primates from the Fayum, Egypt: Implications for diet. *American Journal of Physical Anthropology*, 101, 527–543.
- Teaford, M. F., & Oyen, O. J. (1989). In vivo and in vitro turnover in dental microwear. *American Journal of Physical Anthropology*, 80(4), 447–460. <https://doi.org/10.1002/ajpa.1330800405>
- Teaford, M. F., Ungar, P. S., Taylor, A. B., Ross, C. F., & Vinyard, C. J. (2020). The dental microwear of hard- object feeding in laboratory *Sapajus apella* and its implications for dental microwear formation. *American Journal of Physical Anthropology*, 171(3), 439–455. <https://doi.org/10.1002/ajpa.24000>
- Thiery, G., Gibert, C., Guy, F., Lazzari, V., Geraads, D., Spassov, N., & Merceron, G. (2021). From leaves to seeds? The dietary shift in late Miocene colobine monkeys of southeastern Europe. *Evolution*, 75(8), 1983–1997. <https://doi.org/10.1111/evo.14283>

- Ungar, P. S. (1996). Dental microwear of European Miocene catarrhines: Evidence for diets and tooth use. *Journal of Human Evolution*, 31(4), 335–366. <https://doi.org/10.1006/jhev.1996.0065>
- Ungar, P. S., Brown, C. A., Bergstrom, T. S., & Walker, A. (2003). Quantification of dental microwear by tandem scanning confocal microscopy and scale-sensitive fractal analyses. *Scanning*, 25(4), 185–193. <https://doi.org/10.1002/sca.4950250405>
- Ungar, P. S., Grine, F. E., & Teaford, M. F. (2008). Dental Microwear and Diet of the Plio-Pleistocene Hominin *Paranthropus boisei*. *PLOS ONE*, 3(4), e2044. <https://doi.org/10.1371/journal.pone.0002044>
- Walker, A., Hoeck, H. N., & Perez, L. (1978). Microwear of Mammalian Teeth as an Indicator of Diet. *Science*, 201(4359), 908–910. <https://doi.org/10.1126/science.684415>
- Weber, K., Winkler, D. E., Kaiser, T. M., Žigaitė, Ž., & Tütken, T. (2021). Dental microwear texture analysis on extant and extinct sharks: Ante- or post-mortem tooth wear? *Palaeogeography, Palaeoclimatology, Palaeoecology*, 562, 110147. <https://doi.org/10.1016/j.palaeo.2020.110147>
- Wickham, H., Chang, W., Henry, L., Pedersen, T. L., Takahashi, K., Wilke, C., Woo, K., Yutani, H., Dunnington, D., & RStudio. (2021). *ggplot2: Create Elegant Data Visualisations Using the Grammar of Graphics* (3.3.5) [Computer software]. <https://CRAN.R-project.org/package=ggplot2>
- Williams, V. S., Barrett, P. M., & Purnell, M. A. (2009). Quantitative analysis of dental microwear in hadrosaurid dinosaurs, and the implications for hypotheses of jaw mechanics and feeding. *Proceedings of the National Academy of Sciences*, 106(27), 11194–11199. <https://doi.org/10.1073/pnas.0812631106>
- Winkler, D. E., Kubo, T., Kubo, M. O., Kaiser, T. M., & Tütken, T. (2022). First application of dental microwear texture analysis to infer theropod feeding ecology. *Palaeontology*, 65(6), e12632.
- Winkler, D. E., Schulz-Kornas, E., Kaiser, T. M., Codron, D., Leichliter, J., Hummel, J., Martin, L. F., Clauss, M., & Tütken, T. (2020). The turnover of dental microwear texture: Testing the “last supper” effect in small mammals in a controlled feeding experiment. *Palaeogeography, Palaeoclimatology, Palaeoecology*, 557, 109930. <https://doi.org/10.1016/j.palaeo.2020.109930>

Winkler, D. E., Schulz-Kornas, E., Kaiser, T. M., & Tütken, T. (2019). Dental microwear texture reflects dietary tendencies in extant Lepidosauria despite their limited use of oral food processing. *Proceedings of the Royal Society B: Biological Sciences*, 286(1903), 20190544. <https://doi.org/10.1098/rspb.2019.0544>

629